CHEMISTRY AND TECHNOLOGY OF MEDICINAL COMPOUNDS AND BIOLOGICALLY ACTIVE SUBSTANCES

ХИМИЯ И ТЕХНОЛОГИЯ ЛЕКАРСТВЕННЫХ ПРЕПАРАТОВ И БИОЛОГИЧЕСКИ АКТИВНЫХ СОЕДИНЕНИЙ

ISSN 2686-7575 (Online)

https://doi.org/10.32362/2410-6593-2022-17-4-335-345

UDC 615.28

RESEARCH ARTICLE

Antibacterial activity of green fabricated silver-doped titanates

Anh C. Ha[1,2,✉], Tri Nguyen[3,4], Phung A. Nguyen[3], Van M. Nguyen[4]

[1]*Vietnam National University Ho Chi Minh City, Linh Trung Ward, Thu Duc District, Ho Chi Minh City, Vietnam*
[2]*Faculty of Chemical Engineering, Ho Chi Minh City University of Technology (HCMUT), 268 Ly Thuong Kiet Street, Ho Chi Minh City, Vietnam*
[3]*Institute of Chemical Technology, Vietnam Academy of Science and Technology, 01A TL29 Street, Thanh Loc Ward, District 12, Ho Chi Minh City, Vietnam*
[4]*Ho Chi Minh City Open University, 97 Vo Van Tan Street, District 3, Ho Chi Minh City, Vietnam*
✉*Corresponding author, e-mail: hcanh@hcmut.edu.vn*

Abstract

Objectives. *The study aimed to synthesize the multifunctional materials silver-added titanates via reduction of sol-gel fabricating titanates (Fe_2TiO_5 and $NiTiO_3$) with Jasminium subtriplinerve Blume leaf extract.*
Methods. *The physicochemical characteristics of the obtained materials were determined by X-ray diffraction, energy dispersive X-Ray spectroscopy, Raman spectroscopy, Brunauer–Emmett–Teller specific surface area, scanning electron microscopy, and UV–Vis absorption spectroscopy.*
Results. *The results demonstrated good dispersion of silver on the surface of Fe_2TiO_5 and $NiTiO_3$ to create photocatalysts with two light-absorbing regions. The obtained materials were applied as antibacterial agents in polluted water. The Ag–Fe_2TiO_5 (Ag–FTO) samples showed better properties and antibacterial activity than Ag–$NiTiO_3$ (Ag–NTO) due to the better dispersion of silver nanoparticles on the FTO surface. Besides, the antibacterial results exhibit increased inhibiting activity against gram-negative (−) bacteria as compared with gram-positive (+) bacteria.*

Conclusions. *Nanomaterials Fe_2TiO_5 and $NiTiO_3$ added Ag were successfully synthesized. These materials showed excellent inhibition against Baccilus cereus, Escherichia coli, Pseudomonas aeruginosa, Salmonella typhi, and Staphylococcus aureus. Additionally, the Ag–Fe_2TiO_5 samples showed much better antibacterial activity than the Ag–$NiTiO_3$ sample.*

Keywords: *Iron(III) titanate, nickel titanate, Jasminum subtriplinerve Blume leaf, antibacterial activity*

For citation: Ha C.A., Nguyen T., Nguyen P.A., Nguyen V.M. Antibacterial activity of green fabricated silver-doped titanates. *Tonk. Khim. Tekhnol. = Fine Chem. Technol*. 2022;17(4):335–345. https://doi.org/10.32362/2410-6593-2022-17-4-335-345

НАУЧНАЯ СТАТЬЯ

Антибактериальная активность биосинтетических титанатов, допированных серебром

А.К. Ха[1,2,✉], Т. Нгуен[3,4], П.А. Нгуен[3], В.М. Нгуен[4]

[1]*Вьетнамский национальный университет Хошимина, Линь Чунг Уорд, Район Тхёк, г. Хошимин, Вьетнам*
[2]*Химико-технологический факультет, Технологический университет Хошимина, 268 Ли Тхыонг Кьет ул., г. Хошимин, Вьетнам*
[3]*Химико-технологический институт, Академия наук Вьетнама, 01A TL29 ул., Тха Лог Вард, Район 12, г. Хошимин, Вьетнам*
[4]*Открытый Университет Хошимина, 97, Во Ван Тан ул., Район 3, г. Хошимин, Вьетнам*
✉*Автор для переписки, e-mail: hcanh@hcmut.edu.vn*

Аннотация

Цели. *Синтезировать многофункциональные материалы титанаты с добавлением серебра путем восстановления золь-гелевых производных титанатов (Fe_2TiO_5 и $NiTiO_3$) экстрактом листьев subtriplinerve Blume жасмина.*
Методы. *Физико-химические характеристики полученных материалов определяли методами рентгеновской дифракции, энергодисперсионной рентгеновской спектроскопии, спектроскопии комбинационного рассеяния, удельной поверхности Брунауэра – Эммета – Теллера, сканирующей электронной микроскопия и абсорбционная спектроскопия в УФ-видимой области.*
Результаты. *Результаты показывают, что серебро имеет хорошую дисперсию на поверхности Fe_2TiO_5 и $NiTiO_3$ и создает фотокатализаторы с двумя светопоглощающими областями. Полученные материалы применялись в качестве антибактериальных средств в загрязненных водах. Образцы Ag–Fe_2TiO_5 (Ag–FTO) показали лучшие свойства и антибактериальную активность, чем Ag–$NiTiO_3$ (Ag–NTO) за счет лучшего диспергирования наночастиц серебра на поверхности FTO. Кроме того, антибактериальные результаты демонстрируют большую ингибирующую активность в отношении грамотрицательных (−) бактерий, чем в отношении грамположительных (+) бактерий.*

Выводы. *Успешно синтезированы наноматериалы Fe_2TiO_5 и $NiTiO_3$ с добавлением Ag. Полученные составы показали отличное ингибирование в отношении восковой бациллы (Baccilus cereus), кишечной палочки (Escherichia coli), синегнойной палочки (Pseudomonas aeruginosa), сальмонеллы тифи (Salmonella typhi) и золотистого стафилококка (Staphylococcus aureus). Кроме того, образцы Ag–Fe_2TiO_5 показали гораздо лучшую антибактериальную активность, чем образец Ag–$NiTiO_3$.*

Ключевые слова: *титанат железа(III), титанат никеля, листья subtriplinerve Blume жасмина, антибактериальный*

Для цитирования: Ha C.A., Nguyen T., Nguyen P.A., Nguyen V.M. Antibacterial activity of green fabricated silver-doped titanates. *Tonk. Khim. Tekhnol. = Fine Chem. Technol*. 2022;17(4):335–345. https://doi.org/10.32362/2410-6593-2022-17-4-335-345

INTRODUCTION

The increasing number of industrial production and complex human life activities has seriously affected water quality creating safety concerns. Wastewater contains not only a large number of persistent pollutants but also many dangerous bacteria affecting human health [1, 2]. Therefore, there is an urgent need to overcome these problems, especially in developing countries.

Contemporary treatment methods such as chemical oxidizing agents, chlorination, ultraviolet (UV) radiation, membrane, ozonation, etc., have been considered for water treatment and disinfection purposes [3–5]. Although these methods have demonstrated effectiveness, they also have various disadvantages, such as the creation of toxic byproducts after treatment, high operating costs, and the inability to treat bacteria [3]. The main limitation of catalytic oxidation is the inability to kill bacteria present in wastewater. Semiconductor photocatalytic oxidation is one of the advanced oxidation processes being researched and applied in the wastewater treatment industry.

Although silver (Ag) is well known as a disinfectant against a wide range of bacteria having been widely used in sterilization and bactericidal applications, its practical application is limited due to the ease of oxidation, which can cause aggregation and loss of antimicrobial activity over time. Therefore, Ag requires a supporting substrate to enhance stability of morphological features and maintain antimicrobial efficacy. Therefore, the research aimed at enhancing the antibacterial ability of photocatalyst materials by modifying them or adding another material with antibacterial properties is required.

The widely used TiO_2 semiconductor catalyst has been commercialized as TiO_2-P25. However, its practical application is limited by the large bandgap energy (3.2 eV) and high recombination of electron and hole pairs [6, 7]. Therefore, the modification of TiO_2 structure to improve its catalytic efficiency and stability has been receiving much interest from researchers along with the study of new potential semiconductor materials.

Perovskite-like materials possessing suitable properties, such as chemically inert, high mechanical strength, high absorption coefficient, low activation energy, and significant transparency, are being researched and developed for photocatalytic applications [6, 7]. Among them, titanate-based materials have shown their potential with high activity and stability. Fe_2TiO_5 pseudobrookite has received much attention due to its low band gap energy (1.9–2.2 eV), higher energy level minimum conduction band, superior photochemical stability, and low cost, representing a promising photocatalyst product [8–10]. Another titanate, $NiTiO_3$ perovskite, comprising an n-type semiconductor with an ilmenite-type crystal structure, has attracted considerable attention due to its superior photocatalytic and electro-optical properties and low dielectric constant [11, 12]. $NiTiO_3$ also exhibits an optical absorption

spectrum with band gap energy around 3.0 eV, offering excellent potential for visible light photocatalytic applications [13]. Thus, the Ag-added titanates can be used to create multifunctional composites with excellent photocatalytic antibacterial activity in wastewater. However, there are almost no studies on the addition of Ag to Fe_2TiO_5 and $NiTiO_3$ to enhance their antibacterial ability.

In our research, multifunctional Ag-added titanates (Fe_2TiO_5 and $NiTiO_3$) were synthesized by biosynthesis using *Jasminium subtriplinerve Blume* (JS) leaf extract as a reducing agent of $AgNO_3$ solution to Ag^0, in which Fe_2TiO_5 and $NiTiO_3$ are prepared by the sol-gel method. JS is a member of the Oleaceae genera. Compounds such as triterpenoids, oleanolic acid, flavonoids, glucosides, etc. [14–16], which have been identified and reported in its phytochemicals, can be employed as reducing reagents in the process of biosynthesizing silver nanoparticles. The physicochemical properties of the prepared nanoparticles have been investigated. The antibacterial action of prepared nanoparticles was evaluated with the help of bacteria such as gram-negative *Escherichia coli* (*E. coli*), *Pseudomonas aeruginosa* (*P. aeruginosa*), and *Salmonella typhi* (*Salmonella*), and gram-positive *Baccilus cereus* (*B. cereus*) and *Staphylococcus aureus* (*S. aureus*), which are typically present in wastewater.

MATERIALS AND METHODS

Pseudobookite Fe_2TiO_5 and perovskite $NiTiO_3$ were prepared by sol-gel method according to the procedure described in detail in the works [17, 18], respectively. First, 4.04 g of $Fe(NO_3)_3 \cdot 9H_2O$ (99.9%, *Merck*, Germany) or $Ni(NO_3)_2 \cdot 6H_2O$ (99.9%, *Merck*, Germany) and 2.1 g of $C_6H_8O_7 \cdot H_2O$ (99.9%, *Merck*, Germany) were dissolved with 5 mL of C_2H_5OH (99%, *Merck*, Germany). Next, 3 mL of $Ti(OC_3H_7)_4$ (99.7%, *Merck*, Germany) was added drop by drop. The synthetic gel was dried at 60°C for 24 h and follows by heating at 700°C for 2 h to obtain a Fe_2TiO_5 and $NiTiO_3$ samples.

Ag-doped Fe_2TiO_5 (Ag–FTO) and Ag-doped $NiTiO_3$ (Ag–NTO) catalysts were synthesized using JS leaf extract as a reducing agent of $AgNO_3$ solution to Ag^0. JS leaf was collected from Ho Chi Minh City in Vietnam. After washing and shredding, JS leaf is dried at a temperature of 60°C for 4 h. Next, 50 g of the JS leaf were mixed with 1000 mL of deionized water and heated to 80°C for 2 h under stirring. Finally, the JS leaf extract was filtered and preserved at 4°C for further experiments. Silver nitrate ($AgNO_3$, >99.8%, *Merck*, Germany) was purchased. The optimized conditions for the Ag nanoparticles (AgNPs) synthesis using JS extract as a reducing agent were determined based on our previous publication [16], involving the presence of the light illumination, a synthesis time of 150 min, a volume ratio of $AgNO_3$ solution/JS extract of 18:2, a $AgNO_3$ concentration of 1.0 mM and a stirring rate of 300 rpm at temperature of 20°C. To synthesize Ag–FTO and Ag–NTO, Fe_2TiO_5 and $NiTiO_3$ powders were initially added together in a determined proportion with 1 mM $AgNO_3$ precursor. The samples are denoted as *x*Ag–FTO and *x*Ag–NTO, where *x* represents the silver content added to titanates.

The physicochemical characteristics were studied including X-ray diffraction (XRD), Raman spectroscopy, scanning electron microscopy (SEM), Brunauer–Emmett–Teller adsorption (BET), energy dispersive X-ray spectroscopy (EDS), and UV–Vis absorption spectra techniques. The method of implementation is as detailed in our previous study [19].

The obtained samples have been tested for antibacterial activity against gram-negative *E. coli*, *P. aeruginosa*, and *Salmonella*, and gram-positive *B. cereus* and *S. aureus* by the minimum inhibitory concentration (MIC). These methods have been presented in our previous studies [20].

RESULTS AND DISCUSSION

The XRD pattern (Fig. 1) of the Ag–FTO samples shows mainly diffraction peaks of the pseudobrookite Fe_2TiO_5 at 2θ = 18.2°, 25.7°, 27.6°, 32.7°, 37.5°, 40.6°, 46.3°, 49.0°, 52.5°, and 60.1° (JCPDS[1] card No. 41-1432). In addition, a few other characteristic peaks of rutile with low intensity at 2θ = 27.3°, 36.1°, and 41.5° (JCPDS card No. 21-1276) were observed. There was practically no appearance of characteristic peaks of anatase (JCPDS card No. 21-1272). Some silver peaks with low intensity were also observed for Ag–FTO samples at 2θ = 37.4, 39.0, and 41.1° (JCPDS card No. 04-0783). Diffraction peaks of Ag^0 species were observed more clearly in the 1.0Ag–NTO sample, where Ag concentration was loaded up to 1.0 wt %. The phase composition of the Ag–FTO sample completely coincides with that of the pure Fe_2TiO_5 sample [17], indicating that Ag does not change the phase structure of

[1] JCPDS (Joint Committee on Powder Diffraction Standards)—International Center for Diffraction Data.

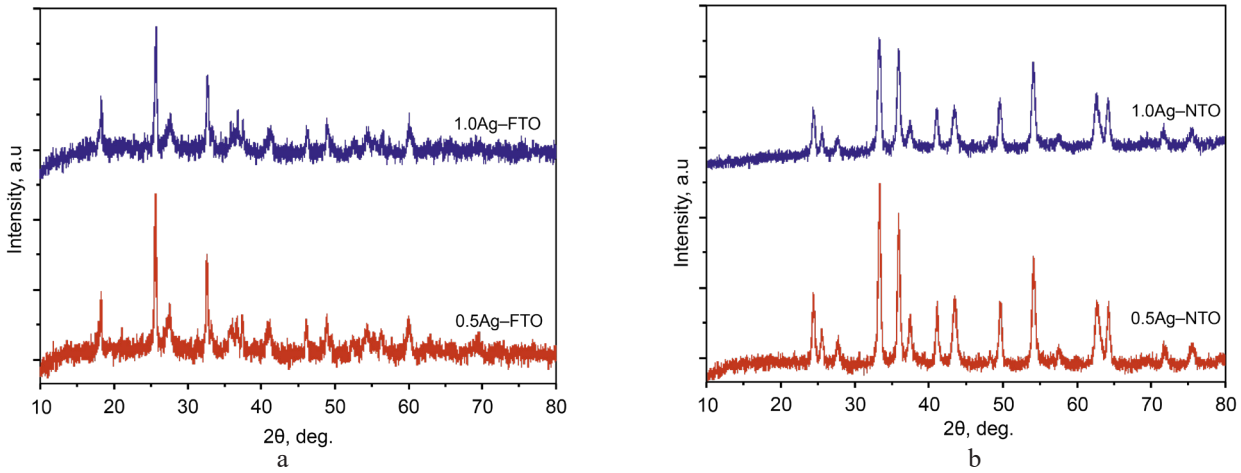

Fig. 1. XRD patterns of Ag–FTO (a) and Ag–NTO (b) catalysts.

pseudobrookite. However, the presence of Ag reduced the crystal size of Fe_2TiO_5 from 31.6 nm to 18.6 nm as calculated based on the Scherrer equation. For the Ag–NTO samples, the peaks of $NiTiO_3$ were observed at 2θ = 23.9°; 32.8°; 35.4°; 53.4°; 61.9°; and 63.5°(JCPDS 75-3757). The XRD spectra of these samples also demonstrated the presence of anatase crystalline phase at 2θ = 25.4° and rutile crystalline phase at 2θ = 27.6°, as well as some characteristic peaks of Ag at 2θ = 37.4, 39.0, and 41.1°. The average crystal size of $NiTiO_3$ is 17–18 nm, which were approximately the same for the Ag–FTO samples. From the XRD diagram, the crystal size of Ag^0 is estimated to be a few nm.

The elemental compositions of the 0.5Ag–FTO and 0.5Ag–NTO samples were determined by EDS analysis. EDS images show that both silver-modified samples have a uniform distribution of Ag crystals on the Fe_2TiO_5 and $NiTiO_3$ surfaces (Fig. 2). In which, the Ag distribution is more

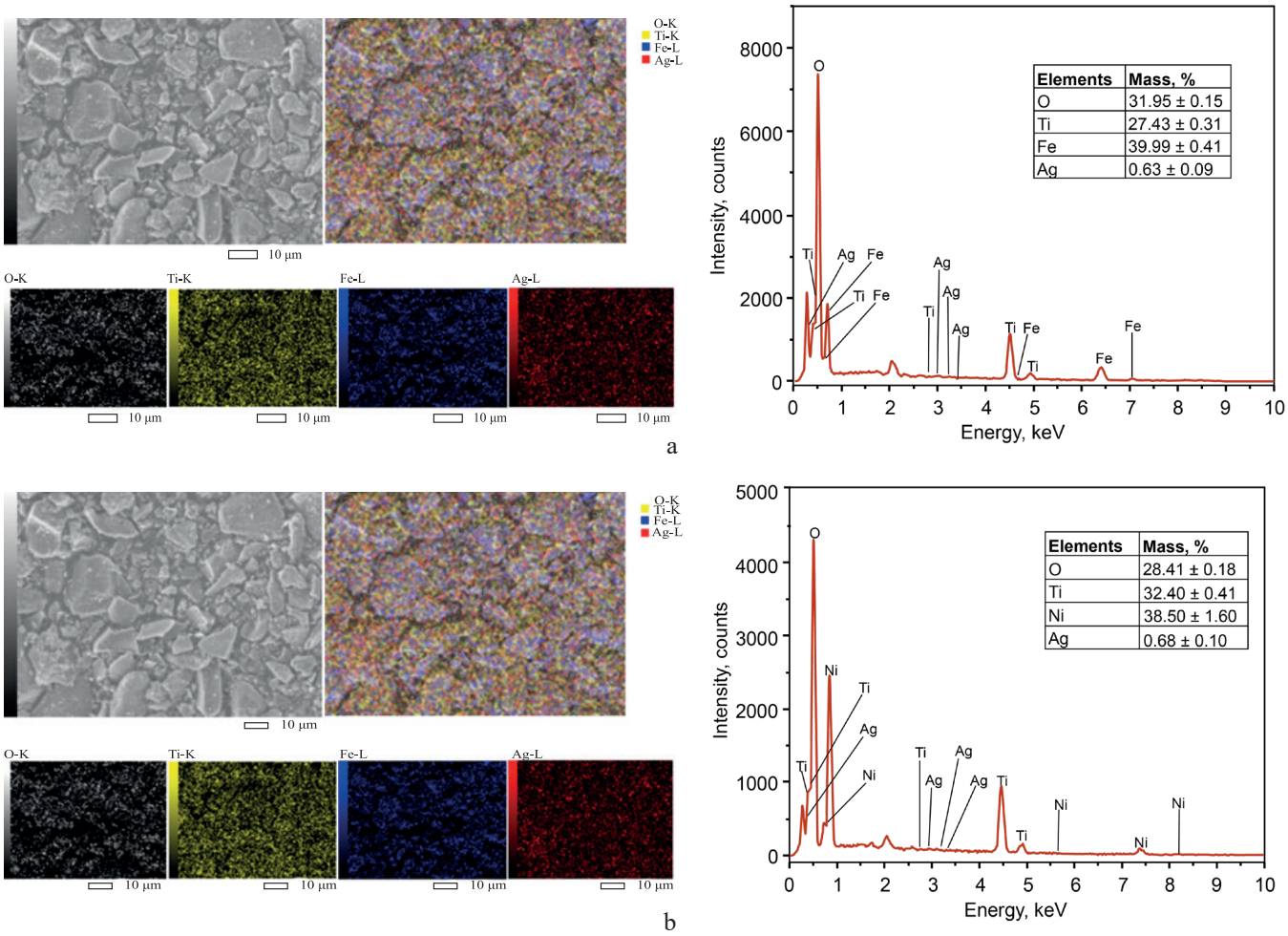

Fig. 2. EDS analysis of 0.5Ag–FTO (a) and 0.5Ag–NTO (b) samples.

dominant for 0.1Ag–FTO sample than that of 0.1Ag–NTO sample. Meanwhile, the EDS spectrum of the 0.1Ag–FTO sample shows the characteristic peaks of Fe, Ti, O, and Ag. The mass ratio of these elements corresponds to 39.99:27.43:31.95:0.63, which is nearly equivalent to the theoretical mass ratio of 0.1Ag–FTO (46.43:19.09:33.17:0.50). The EDS spectrum of sample 0.1Ag–NTO also shows characteristic peaks of Ni, Ti, O, and Ag with mass ratios 38.50:32.40:28.41:0.68, respectively. This ratio is also quite close to the theoretical mass ratio of 0.1Ag–NTO (37.78:30.82:30.90:0.50). Comparing 0.1Ag–FTO and 0.1Ag–NTO samples, the 0.1Ag–FTO sample seems to have a more similar experimental mass ratio of elements and theoretical mass ratio than that of 0.1Ag–NTO, demonstrating the higher purity of this sample. In addition, some unassigned peaks on the EDS spectra of both samples were characteristic peaks of the carbon tape material covering the samples. From the EDS and XRD results, it can be concluded that the silver was formed and uniformly dispersed on the surface as well as inside the structure of Fe_2TiO_5 and $NiTiO_3$.

The Raman spectrum of Ag–FTO samples (Fig. 3) shows the appearance of absorption peaks characteristic for Fe_2TiO_5 structure at 144 cm^{-1}, 199 cm^{-1}, 222 cm^{-1}, 292 cm^{-1}, 327 cm^{-1}, 394 cm^{-1}, 661 cm^{-1}, 787 cm^{-1}, and 1294 cm^{-1} [21]. Here, the characteristic Ag oscillations at 199, 327, and 787 cm^{-1} correspond to the strain vibration in the inner plane of the O–Ti bond, the symmetric stretching vibration of the O–Fe bond, and the symmetrical bending vibrations of the O–Ti bond. Meanwhile, the B_{1g} oscillations at 144 cm^{-1}, 222 cm^{-1}, and 661 cm^{-1} are formed by the out-of-plane rotation of the O–Ti bond, bending vibrations in the plane of the O–Fe bond, and external bending vibrations of the Ti–O bond, respectively. Moreover, the characteristic peaks of Fe_2O_3 are not significantly present in the Raman spectrum. Therefore, this result proves that the obtained Fe_2TiO_5 has high crystallinity with a stable phase structure. Meanwhile, for Ag–NTO samples, the Raman vibrational modes for $NiTiO_3$ are located at 192 cm^{-1} (A_g), 229 cm^{-1} (B_g), 246 cm^{-1} (A_g), 291 cm^{-1} (B_g), 345 cm^{-1} (B_g), 394 cm^{-1} (A_g), 465 cm^{-1} (B_g), 484 cm^{-1} (A_g), 613 cm^{-1} (B_g), and 709 cm^{-1} (B_g). The characteristic A_g and B_g oscillations correspond to the strain vibration in the inner plane of the O–Ti bond, symmetrical bending vibrations of the O–Ti bond, and the symmetric stretching vibration of the O–Ni bond. Since the Raman spectrum shows almost no characteristic oscillations of Ag for both Ag–FTO and Ag–NTO samples, it can be concluded that silver is present in low concentrations and well dispersed on the surface of Fe_2TiO_5 and $NiTiO_3$.

SEM images (Fig. 4) show that the Ag–FTO and Ag–NTO materials exist in the form of small quasi-spherical particles and large bulk. For both Ag–FTO and Ag–NTO samples, samples containing 0.5% Ag exhibited less agglomeration, smaller clumps, and better dispersion of brightly colored spherical Ag particles. This means that there will be better porosity for bacteria location and conversion.

Figure 5a shows the N_2 adsorption-desorption isotherms of 0.5Ag–FTO and 0.5Ag–NTO samples. According to the IUPAC nomenclature [22], the shape of the nitrogen isotherm of two samples could be considered to be a type IV isotherm, which is typical for mesoporous materials. Here, the width of the hysteresis loop of the Ag–FTO sample is much higher than that of the Ag–NTO sample, demonstrating the better adsorption capacity of this material for bacteria. The curve of

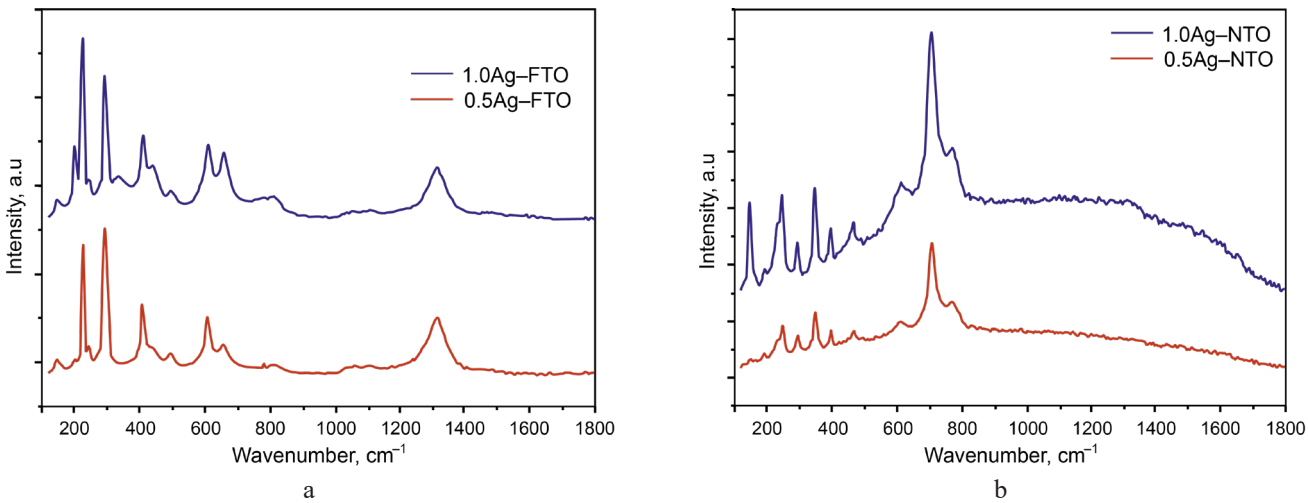

Fig. 3. Raman spectra of Ag–FTO (a) and Ag–NTO (b) catalysts.

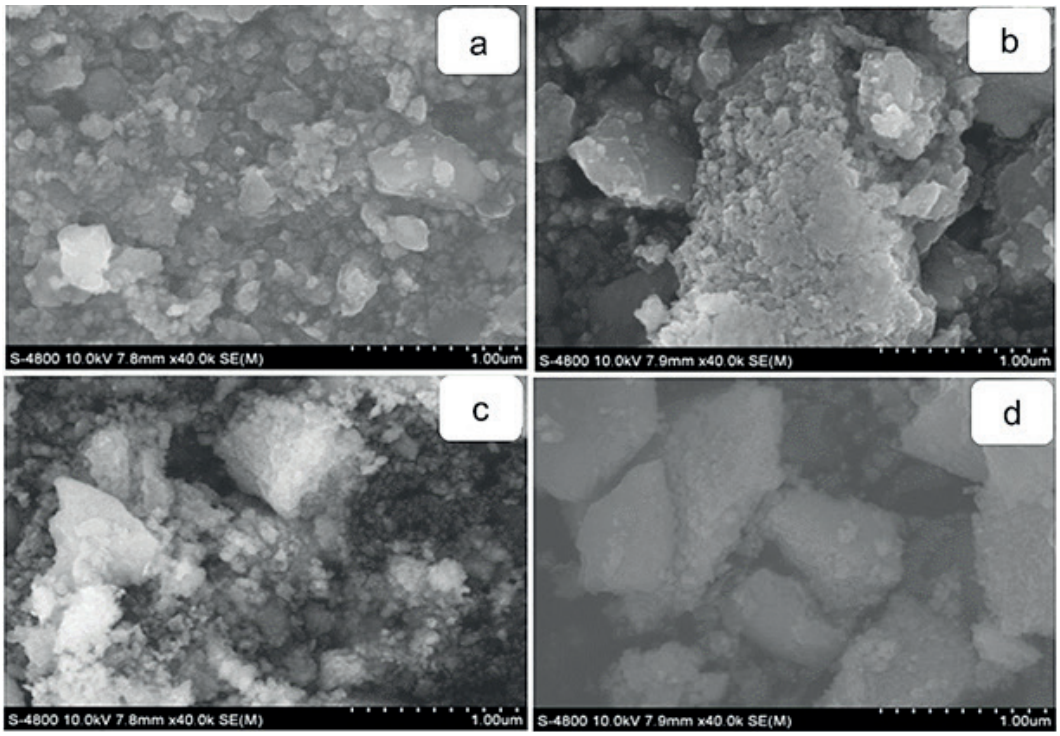

Fig. 4. SEM images of samples: 0.5Ag–FTO (a), 1.0Ag–FTO (b), 0.5Ag–NTO (c), 1.0Ag–NTO (d).

the pore size distribution of the 0.5Ag–FTO and 0.5Ag–NTO samples according to their diameters additionally allowed the maximum diameter densities of 24.0 Å and 23.4 Å, respectively, to be determined (Fig. 5b). These were used to calculate the BET data for 0.5Ag–FTO and 0.5Ag–NTO samples. For the 0.5Ag–FTO sample, the specific surface area of the examined sample was 20.2 m^2/g, while the total pore volume was found to be 0.025 cm^3/g. Meanwhile, these values reach 13.8 m^2/g and 0.017 cm^3/g for the 0.1Ag–NTO sample, respectively. These results demonstrate that Ag–FTO has better adsorption capacity than the Ag–NTO.

The absorbed wavelength and the band gap energy of the catalysts were determined by UV–Vis spectroscopy and the Tauc plot. The obtained results show that there is almost no difference in absorption wavelength and band gap between Ag-added samples. Specifically, for the Ag–FTO samples (Fig. 6a), it can be seen that the absorbed light band and band gap energy form two different regions: the first region has an absorption wavelength range in the range of 630−633 nm corresponding to a band gap energy of 1.96−1.97 eV. The second region has an absorption wavelength range of 493−496 nm corresponding to a band gap energy of 2.50−2.52 eV.

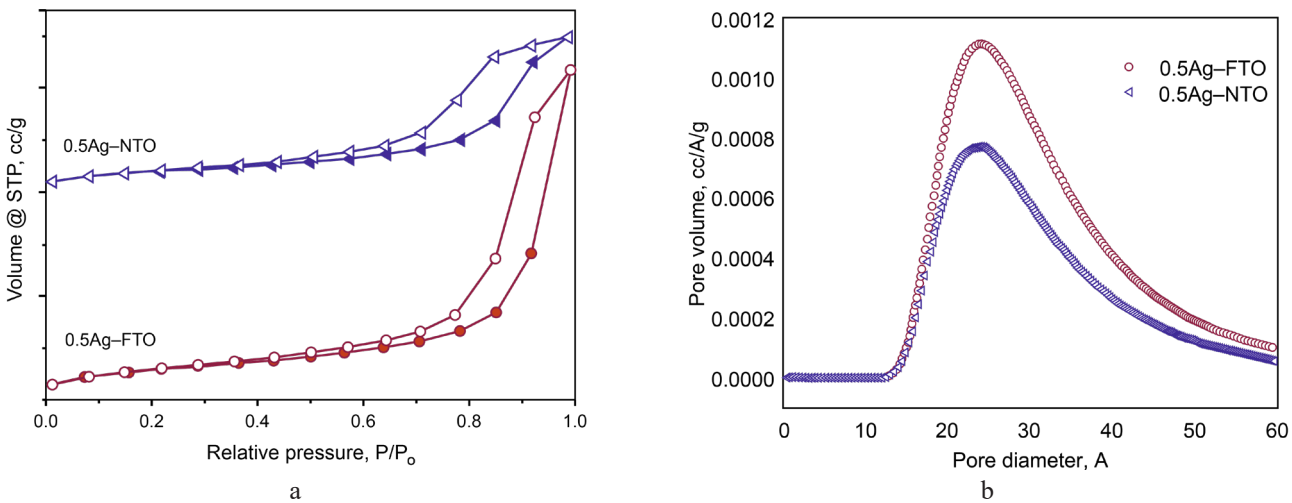

Fig. 5. N_2 adsorption-desorption isotherms (a) and pore size distribution (b) of 0.5Ag–FTO and 0.5Ag–NTO samples.

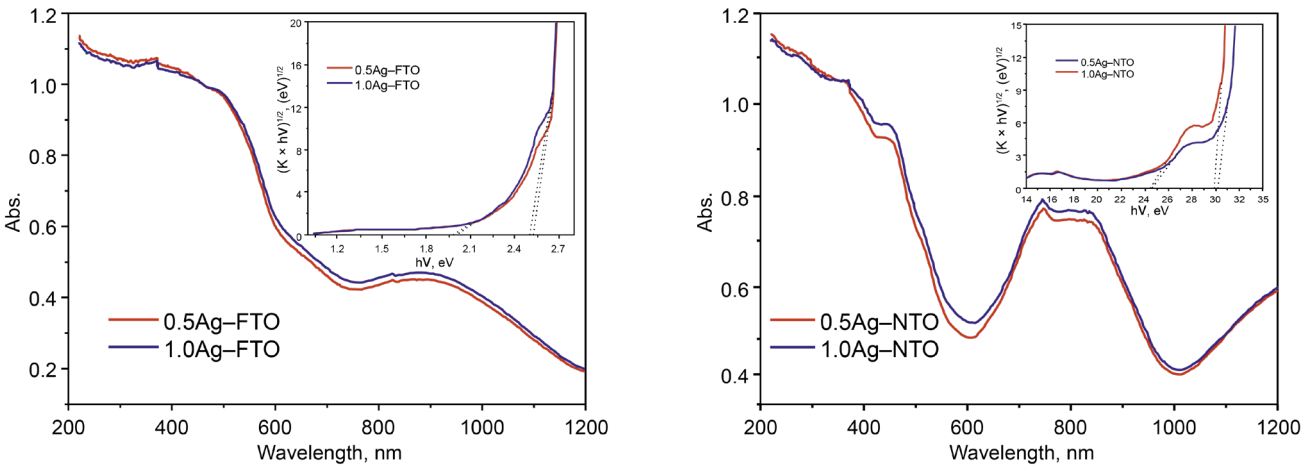

a b

Fig. 6. UV–Vis diffuse reflectance spectra and Tauc plot of the Ag–FTO (a) and Ag–NTO (b) samples.

According to previous studies [8–10], Fe_2TiO_5 has a band gap energy of 1.9−2.1 eV (corresponding to an absorption wavelength of about 590−650 nm), which is consistent with the first band data; meanwhile, silver has an absorption wavelength in the range of 400−500 nm (band gap energy in the range of 2.4−3.1 eV) [23], which is consistent with the second band parameters. The appearance of two absorption wavelength regions and band gap energies is similar for Ag–NTO samples (Fig. 6b). In which, the first region corresponds to 411–414 nm and 3.0–3.02 eV; and the second region is 504–406 nm and 2.45–2.46 eV, respectively. According to author [13], $NiTiO_3$ has a band gap energy of about 3.0 eV, which is consistent with the first band results of the catalysts, while the second is also compatible with the absorption region of silver. It can be concluded that the combination of silver with Fe_2TiO_5 and $NiTiO_3$ leads to the appearance of a smaller frequency band, which increases flexibility in the light absorption of the material. It can be found that the Ag–FTO materials with bandgap absorb light and bandgap better than the Ag–NTO samples. This is an essential property of photocatalyst materials, which can lead to their improved activity.

The antibacterial properties of the samples were determined by their minimum inhibitory concentration (MIC). Five types of bacterial including *E. coli*, *P. aeruginosa*, *Salmonella*, and *S. aureus* were used in this study. The exponential phase of bacteria was observed to be delayed in the presence of samples; this phenomenon was more obvious with the rise of Ag–FTO and Ag–NTO concentrations (Fig. 7). The samples were able to inhibit the exponential stage of both gram-negative and gram-positive bacteria. The MIC against *B. cereus*, *E. coli*, *P. aeruginosa*, *Salmonella*, and *S. aureus* of Ag–FTO and Ag–NTO samples are described in Table. Here it can be seen that the 0.5Ag–FTO were able to completely inhibit the growth of *B. cereus*, *E. coli*, *P. aeruginosa*, *Salmonella*, and *S. aureus* at a similar MIC of 1.25, 0.31, 1.25, 1.25, and 2.50 μg/mL, respectively. The almost doubled MIC value when increasing the silver content up to 1.0% for the Fe_2TiO_5 samples (1.0Ag–FTO) demonstrates their enhanced antimicrobial activity with the addition of silver. Meanwhile, the antibacterial ability of 0.5Ag–NTO proved to be lower than that of 0.5Ag–FTO with MIC values of 5.00, 2.50, 2.50, 2.50, and 5.00 μg/mL respectively. A similar phenomenon was observed for the 1.0Ag–FTO sample with an improvement in antibacterial activity with increasing Ag concentration. It is clear that the Ag–FTO samples exhibit much higher antibacterial activity than Ag–NTO due to the better dispersion of silver nanoparticles on the Fe_2TiO_5 surface (shown by their physicochemical properties). The synthesized samples in this study were shown to be more effective against the negative bacterial (*E. coli*, *Salmonella*, and *P. aeruginosa*) as compared to the positive bacterial (*B. cereus* and *S. aureus*). These results were the agreement with previous reports [24, 25] when assuming that the gram-negative bacteria had thinner cell walls than the gram-positive bacteria; thus, the antibacterial materials can more easily penetrate and inhibit gram-negative bacteria.

As compared to some similar earlier reported materials, the obtained materials exhibit superior antibacterial ability. Specifically, silver nanoparticles (AgNPs) synthesized using *Acalypha indica* leaf extract had an MIC of 10 μg/mL against *E. coli* and *Vibrio cholera* (*V. cholera*) [26], while $LaAlO_3$ perovskite nanoparticles had an MIC of 63 μg/mL against gram-negative bacteria *P. aeruginosa* [27] and

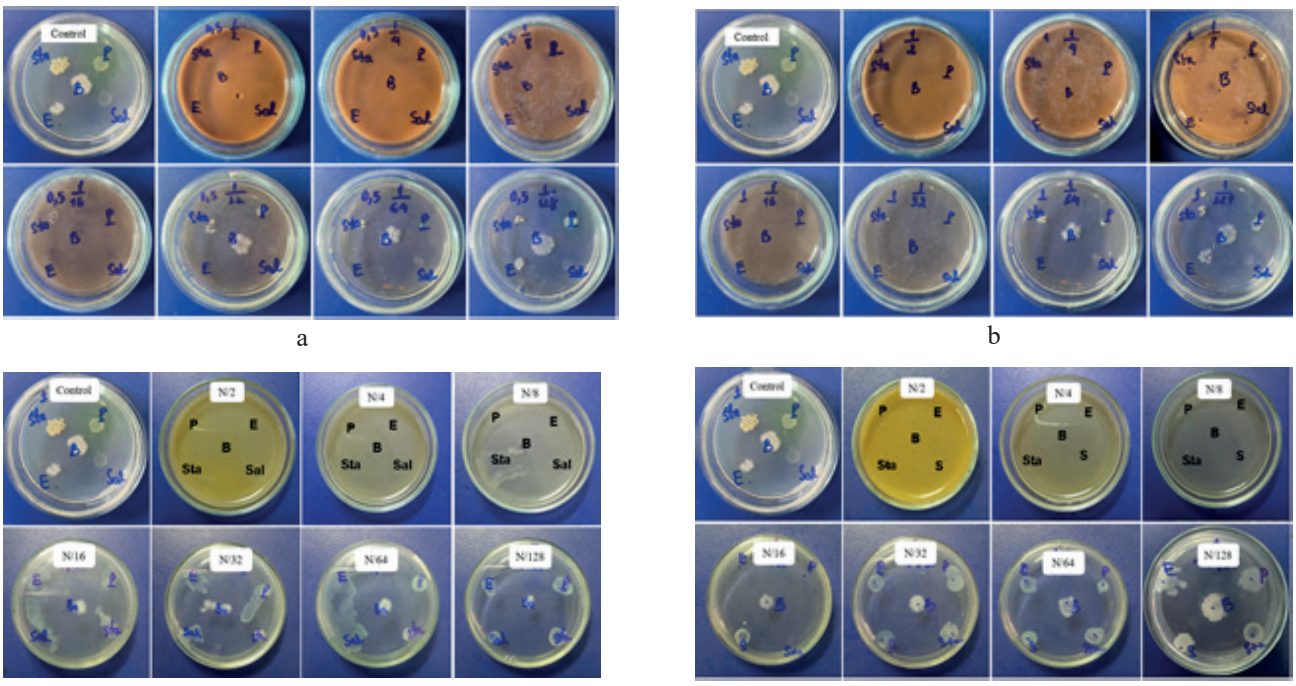

Fig. 7. Minimum inhibitory concentrations of 0.5Ag–FTO (a), 1.0Ag–FTO (b), 0.5Ag–NTO (c), 1.0Ag–NTO (d) samples against five bacteria.

Table. Minimum inhibitory concentrations (MIC) on samples against five bacteria

Bacteria	MIC (μg/mL)			
	0.5Ag–FTO	1.0Ag–FTO	0.5Ag–NTO	1.0Ag–NTO
Baccilus cereus	1.25	0.63	5.00	2.50
Escherichia coli	0.31	0.31	2.50	1.25
Pseudomonas aeruginosa	1.25	0.63	2.50	1.25
Salmonella tophi	1.25	0.63	2.50	1.25
Staphylococcus aureus	2.50	1.25	5.00	2.50

the modified perovskite material $LaCo_{0.4}Fe_{0.6}O_3$ showed an MIC of 63 μg/mL against two bacteria *S. aureus* and *P. aeruginosa* [28]. Studies on perovskite materials and silver nanoparticles have shown effective bactericidal ability against both gram-negative and gram-positive bacteria. Perovskite-like materials combined with silver not only release metal ions Fe^{3+}, Ni^{2+}, Ti^{+4} but also Ag^{+} ions having a positive charge, causing electrostatic attraction with negative charge of bacterial cell membrane. As a consequence, ionic particles easily adhere to cell walls and membranes, changing the membrane structure to destroy the bacterial cell [29, 30].

CONCLUSIONS

In summary, Ag-added Fe_2TiO_5 and $NiTiO_3$ nanomaterials were successfully synthesized by biosynthesis combined with the sol-gel method. Well-distributed silver nanoparticles on Fe_2TiO_5 and $NiTiO_3$ surfaces on a nanoscale and with a low band gap were observed for the samples. The antibacterial efficacy of Ag–FTO and Ag–NTO samples has been demonstrated through excellent inhibition against *B. cereus*, *E. coli*, *P. aeruginosa*, *Salmonella*, and *S. aureus* with the low MIC minimum inhibitory concentration due to the excellent dispersion of Ag on the surface of the perovskite. At the same time, the Ag–FTO samples also showed much better antibacterial activity than the Ag–NTO samples as a result of the excellent dispersion of Ag on the Fe_2TiO_5 surface. Hence, according to the findings of this research, the use of Ag–FTO nanomaterials may suggest potential applications in disinfection and sterilization applications in future wastewater treatment approaches.

Acknowledgments

We acknowledge the support of time and facilities from Ho Chi Minh University of Technology (HCMUT), VNU-HCM for this study.

Благодарности

Авторы благодарят Технологический университет Хо Ши Мина за поддержку в этом исследовании.

Authors' contribution

All authors equally contributed to the research work.

Вклад авторов

Все авторы в равной степени внесли свой вклад в исследование.

The authors declare no conflicts of interest.
Авторы заявляют об отсутствии конфликта интересов.

REFERENCES

1. Xiang W., *et al*. Biochar technology in wastewater treatment: A critical review. *Chemosphere*. 2020;252:126539. https://doi.org/10.1016/j.chemosphere.2020.126539

2. Yaqoob A.A., Parveen T., Umar K., Mohamad Ibrahim M.N. Role of nanomaterials in the treatment of wastewater: A review. *Water*. 2020;12(2):495. https://doi.org/10.3390/w12020495

3. Crini G., Lichtfouse E. Advantages and disadvantages of techniques used for wastewater treatment. *Environ. Chem. Lett*. 2019;17(1):145–155. https://doi.org/10.1007/s10311-018-0785-9

4. Salgot M., Folch M. Wastewater treatment and water reuse. *Curr. Opin. Environ. Sci. Health*. 2018;2:64–74. https://doi.org/10.1016/j.coesh.2018.03.005

5. Rizzo L., *et al*. Best available technologies and treatment trains to address current challenges in urban wastewater reuse for irrigation of crops in EU countries. *Sci. Total Environ*. 2020;710:36312. https://doi.org/10.1016/j.scitotenv.2019.136312

6. Dai Y., Poidevin C., Ochoa-Hernández C., Auer A.A., Tüysüz H. A supported bismuth halide perovskite photocatalyst for selective aliphatic and aromatic C–H bond activation. *Angew. Chemie Int. Ed*. 2020;59(14):5788–5796. https://doi.org/10.1002/anie.201915034

7. Kanhere P., Chen Z. A review on visible light active perovskite-based photocatalysts. *Molecules*. 2014;19(12):19995–20022. https://doi.org/10.3390/molecules191219995

8. Nikolic M., Lukovic M., Vasiljevic Z., Labus N., Aleksic O. Humidity sensing potential of Fe_2TiO_5–pseudobrookite. *J. Mater. Sci.: Mater. Electron*. 2018:29(11):9227–9238. https://doi.org/10.1007/s10854-018-8951-1

9. Thambiliyagodage C., Mirihana S., Wijesekera R., Dinu S.M., Kandanapitiye M., Bakker M. Fabrication of Fe_2TiO_5/TiO_2 binary nanocomposite from natural ilmenite and their photocatalytic activity under solar energy. *Curr. Res. Green Sustain. Chem*. 2021;4:100156. https://doi.org/10.1016/j.crgsc.2021.100156

10. Lou Z., Li Y., Song H., Ye Z., Zhu L. Fabrication of Fe_2TiO_5/TiO_2 nanoheterostructures with enhanced visible-light photocatalytic activity. *RSC Advances*. 2016;6(51):45343–45348. https://doi.org/10.1039/C6RA06763H

11. Lakhera S.K., *et al*. Enhanced photocatalytic degradation and hydrogen production activity of *in situ* grown TiO_2 coupled $NiTiO_3$ nanocomposites. *Appl. Surf. Sci*. 2018:449:790–798. https://doi.org/10.1016/j.apsusc.2018.02.136

12. Li H., Huang W., Wang G.-L., Wang W.-L., Cui X., Zhuang J. Transcriptomic analysis of the biosynthesis, recycling, and distribution of ascorbic acid during leaf development in tea plant (*Camellia sinensis* (L.) O. Kuntze). *Sci. Rep*. 2017;7(1):46212. https://doi.org/10.1038/srep46212

13. Xing C., *et al*. Porous $NiTiO_3/TiO_2$ nanostructures for photocatatalytic hydrogen evolution. *J. Mater. Chem. A*. 2019;7(28):17053–17059. https://doi.org/10.1039/C9TA04763H

14. Ngan D.H., Hoai H.T.C., Huong L.M., Hansen P.E., Vang O. Bioactivities and chemical constituents of a Vietnamese medicinal plant Che Vang, Jasminum subtriplinerve Blume (Oleaceae). *Nat. Prod. Res*. 2008:22(11):942–949. https://doi.org/10.1080/14786410701647119

15. Nguyen T.M.-T., *et al*. Novel biogenic silver nanoparticles used for antibacterial effect and catalytic degradation of contaminants. *Res. Chem. Intermed*. 2020;46(3):1975–1990. https://doi.org/10.1007/s11164-019-04075-w

16. Nguyen P.A., *et al*. Sunlight irradiation-assisted green synthesis, characteristics and antibacterial activity of silver nanoparticles using the leaf extract of *Jasminum subtriplinerve Blume*. *J. Plant Biochem. Biotechnol*. 2022;31:202–205. https://doi.org/10.1007/s13562-021-00667-z

17. Nguyen P.A., *et al*. Envirronmentally friendly fabrication of Fe_2TiO_5-TiO_2 nanocomposite for enhanced photodegradation of cinnamic acid solution. *Adv. Natural Sci.: Nanosci. Nanotechnol*. 2022;12(4):045015. https://doi.org/10.1088/2043-6262/ac498d

18. Nguyen P.A., *et al*. Exceptional photodecomposition activity of heterostructure $NiTiO_3$–TiO_2 catalyst. *J. Sci.: Adv. Mater. Dev*. 2022;7(1):100407. https://doi.org/10.1016/j.jsamd.2021.100407

19. Nguyen D.T., Ha C.A., Nguyen T., Phuong P.H., Hoang T.C. A low temperature fabrication and photoactivity of Al_2TiO_5 in cinnamic acid degradation. *Mater. Trans*. 2019;60(9):2022–2027. https://doi.org/10.2320/matertrans.M2019076

20. Nguyen P.A., Duong N.L., Nguyen V.M., Nguyen T. Positive effects of the ultrasound on biosynthesis, characteristics and antibacterial activity of silver nanoparticles using *Fortunella Japonica*. *Mater. Trans*. 2019;60(9):2053–2058. https://doi.org/10.2320/matertrans.M2019065

21. Rodrigues J.E., *et al*. Spin-phonon coupling in uniaxial anisotropic spin-glass based on Fe_2TiO_5 pseudobrookite. J. Alloys Comp. 2019;799:563–572. https://doi.org/10.1016/j.jallcom.2019.05.343

22. Burhan M., Shahzad M.W., Ng K.C. Energy distribution function based universal adsorption isotherm model for all types of isotherm. *Int. J. Low-Carbon Technol.* 2018;13(3):292–297. https://doi.org/10.1093/ijlct/cty031

23. Barone P., Stranges F., Barberio M., Renzelli D., Bonanno A., Xu F. Study of Band Gap of Silver Nanoparticles–Titanium Dioxide Nanocomposites. *J. Chem*. 2014;2014:589707. http://dx.doi.org/10.1155/2014/589707

24. Ankanna S., Prasad T.N.V.K.V., Elumalai E., Savithramma N. Production of biogenic silver nanoparticles using Boswellia ovalifoliolata stem bark. *Dig. J. Nanomater. Biostruct*. 2010;5(2):369–372.

25. Morones J.R., *et al*. The bactericidal effect of silver nanoparticles. *Nanotechnology*. 2005;16(10):2346–2353. https://doi.org/10.1088/0957-4484/16/10/059

26. Krishnaraj C., *et al*. Synthesis of silver nanoparticles using *Acalypha indica* leaf extracts and its antibacterial activity against water borne pathogens. *Colloids Surf. B: Biointerfaces*. 2010;76(1):50–56. https://doi.org/10.1016/j.colsurfb.2009.10.008

27. Manjunatha C. *et al*. Perovskite lanthanum aluminate nanoparticles applications in antimicrobial activity, adsorptive removal of Direct Blue 53 dye and fluoride. *Mater. Sci. Eng.: C Mater. Biol. Appl*. 2019;101:674–685. https://doi.org/10.1016/j.msec.2019.04.013

28. Singh C., Wagle A., Rakesh J.V. Doped $LaCoO_3$ perovskite with Fe: A catalyst with potential antibacterial activity. *Vacuum*. 2017;146:468–473. https://doi.org/10.1016/j.vacuum.2017.06.039

29. Dakal T.C., Kumar A., Majumdar R.S., Yadav V. Mechanistic basis of antimicrobial actions of silver nanoparticles. *Front. Microbiol*. 2016;7:1831. https://doi.org/10.3389/fmicb.2016.01831

30. Yin I.X., Zhang J., Zhao I.S., Mei M.L., Li Q., Chu C.H. The antibacterial mechanism of silver nanoparticles and its application in dentistry. *Int. J. Nanomedicine*. 2020;15:2555–2562. https://doi.org/10.2147/IJN.S246764

About the Authors:

Anh C. Ha, PhD, Doctor of Medicinal Chemistry, Faculty of Chemical Engineering, Ho Chi Minh City University of Technology (268 Ly Thuong Kiet Street, District 10, Ho Chi Minh City, Vietnam); Vietnam National University Ho Chi Minh City (Linh Trung Ward, Thu Duc District, Ho Chi Minh City, Vietnam). E-mail: hcanh@hcmut.edu.vn. https://orcid.org/0000-0001-7919-4028

Tri Nguyen, PhD, Doctor of Chemical Engineering, Institute of Chemical Technology, Vietnam Academy of Science and Technology (01A TL29 Street, Thanh Loc Ward, District 12, Ho Chi Minh City, Vietnam); Ho Chi Minh City Open University (97 Vo Van Tan Street, District 3, Ho Chi Minh City, Vietnam). E-mail: ntri@ict.vast.vn. https://orcid.org/0000-0001-9486-5096

Anh Ph. Nguyen, Master of Chemical Engineering, Institute of Chemical Technology, Vietnam Academy of Science and Technology (01A TL29 Street, Thanh Loc Ward, District 12, Ho Chi Minh City, Vietnam). Email: npanh@ict.vast.vn. https://orcid.org/0000-0002-5816-9832

Minh V. Nguyen, Master of Biotechnology, Ho Chi Minh City Open University (97 Vo Van Tan Street, District 3, Ho Chi Minh City, Vietnam). E-mail: minh.nv@ou.edu.vn. https://orcid.org/0000-0002-1615-4966

Об авторах:

Ань К. Ха, PhD, к.фарм.н., Химико-технологический факультет, Технологический университет Хошимина (268 Ли Тхыонг Кьет ул., Район 10, г. Хошимин, Вьетнам); Вьетнамский национальный университет Хошимина (Линь Чунг Уорд, Район Тхёк, г. Хошимин, Вьетнам). E-mail: hcanh@hcmut.edu.vn. https://orcid.org/0000-0001-7919-4028

Три Нгуен, PhD, к.т.н., Химико-технологический институт, Академия наук Вьетнама, (01A TL29 ул., Тха Лог Вард, Район 12, г. Хошимин, Вьетнам); Открытый Университет Хошимина (97, Во Ван Тан ул., Район 3, г. Хошимин, Вьетнам). E-mail: ntri@ict.vast.vn. https://orcid.org/0000-0001-9486-5096

Ань Ф. Нгуен, магистр химической технологии, Химико-технологический институт, Академия наук Вьетнама, (01A TL29 ул., Тха Лог Вард, Район 12, г. Хошимин, Вьетнам). E-mail: npanh@ict.vast.vn. https://orcid.org/0000-0002-5816-9832

Минх В. Нгуен, магистр биотехнологии, Открытый Университет Хошимина (97, Во Ван Тан ул., Район 3, г. Хошимин, Вьетнам). E-mail: minh.nv@ou.edu.vn. https://orcid.org/0000-0002-1615-4966

The article was submitted: April 18, 2022; approved after reviewing: May 31, 2022; accepted for publication: August 03, 2022.

The text was submitted by the authors in English
Edited for English language and spelling by Thomas Beavitt